Quantitative NMR analysis of the protein G B1 domain in *Xenopus laevis* egg extracts and intact oocytes

Philipp Selenko*†, Zach Serber‡, Bedrick Gadea§¶, Joan Ruderman†§, and Gerhard Wagner*†

Departments of *Biological Chemistry and Molecular Pharmacology and §Cell Biology, Harvard Medical School, 240 Longwood Avenue, Boston, MA 02115; and ‡Department of Molecular Pharmacology, Stanford University Medical School, 269 West Campus Drive, Stanford, CA 94305

Contributed by Joan Ruderman, June 11, 2006

We introduce a eukaryotic cellular system, the *Xenopus laevis* oocyte, for in-cell NMR analyses of biomolecules at high resolution and delineate the experimental reference conditions for successful implementations of *in vivo* NMR measurements in this cell type. This approach enables quantitative NMR experiments at defined intracellular concentrations of exogenous proteins, which is exemplified by the description of in-cell NMR properties of the protein G B1 domain (GB1). Additional experiments in *Xenopus* egg extracts and artificially crowded *in vitro* solutions suggest that for this biologically inert protein domain, intracellular viscosity and macromolecular crowding dictate its *in vivo* behavior. These contributions appear particularly pronounced for protein regions with high degrees of internal mobility in the pure state. We also evaluate the experimental limitations of this method and discuss potential applications toward the *in situ* structural characterization of eukaryotic cellular activities.

in-cell | high-resolution | liquid-state

Structural investigations of biomolecules are typically confined to artificial and isolated *in vitro* experimental setups. To study proteins in their native environment, i.e., within cells, recent attempts have aimed at the development of *in vivo* techniques for structural biology (1). X-ray crystallography and cryo-electron microscopy are intrinsically restricted from *in vivo* approaches because of their requirement for crystalline or vitrified specimens. NMR spectroscopy, the only other method for structural investigations at the atomic level, allows for the direct and selective observation of NMR-active nuclei within any NMR-inactive environment and can thus be used to structurally investigate labeled proteins inside living cells (2, 3). To date, all applications of in-cell NMR spectroscopy have been conducted in bacterial cells. High-resolution *in vivo* NMR experiments have been reported for the structural and functional characterization of cellular proteins (4–8), protein dynamics (9), and protein–protein interactions (10). Here, we have used intact *Xenopus laevis* oocytes to develop the first eukaryotic cellular system for intracellular NMR analyses of biomolecules at high resolution and at close-to-physiological levels of intracellular sample concentrations.

Xenopus oocytes have long served as important laboratory tools in cellular and developmental biology (11–13). Their large size renders them suitable for microinjection and permits the precise cytoplasmic deposition of defined amounts of labeled, NMR-active proteins into an otherwise unlabeled, native cellular environment. This ensures quantitative sample delivery and a higher degree of reproducibility of *in vivo* measurements than is generally achievable by prokaryotic in-cell NMR methods, which overexpress labeled protein and conduct measurements within the same cells. Moreover, because labeled recombinant proteins are produced in *Escherichia coli* and conventionally purified before injection into oocytes, any background labeling artifacts from endogenous small molecules containing NMR-active isotopes introduced into the cellular environment are eliminated. Another advantage of this system is that crude extracts of *Xenopus* eggs are easily prepared. These extracts closely resemble the undiluted cytoplasmic fraction of intact cells in terms of macromolecular composition, biological activity, and intracellular viscosity. They are widely used as *ex vivo* tools to mimic certain cellular activities or recapitulate specific biological processes (14–16) and provide means to conveniently assess "cellular" NMR properties in a homogenous cell-free solution.

Here, we present a quantitative analysis of how the cellular properties of the protein GB1 domain, at varying intracellular concentrations, relate to experimental parameters obtained for the pure protein, for GB1 in *Xenopus* egg extracts, and in macromolecular crowded *in vitro* solutions. Our data indicate the overall experimental feasibility of in-cell NMR measurements in living, intact *Xenopus* oocytes and describe the quantitative contribution of intracellular viscosity and macromolecular crowding to GB1s *in vivo* behavior. In summary, we provide the methodological reference-frame for high-resolution NMR measurements in a eukaryotic cellular setting, which we hope will enable structural analyses of biological activities typically encountered in higher organisms.

Results

We deliberately chose the biologically inert, streptococcal protein G B1 domain (GB1, 56 residues, 7 kDa) (17) to define the overall experimental reference conditions for in-cell NMR measurements in *X. laevis* oocytes. This model polypeptide, rather than a functional protein, allowed us to accurately deduce the physical properties of the intracellular environment toward a folded protein structure without compromising the quantitative nature of the experimental results by intracellular binding events or other sorts of biological activities. GB1 was expressed and purified in a ^{15}N-labeled form from *E. coli*. Reference proton-nitrogen correlation spectra of pure GB1 were recorded at sample concentrations of 10–500 μM. We began our cellular analyses by resuspending equimolar quantities of labeled GB1 in crude *Xenopus* egg extracts (Fig. 1*A*). *Xenopus* eggs are conveniently laid by hormone-treated female frogs and more readily accessible for extract preparations than oocytes, which have to be surgically removed from ovary lobes and manually selected to yield oocyte extracts. Despite the high abundance of endogenous, unlabeled proteins (>70 mg/ml), the resulting correlation spectra of GB1 in egg extracts were perfectly superimposable with reference spectra of the pure protein (Fig. 1*B*). Changes in

Conflict of interest statement: No conflicts declared.

Freely available online through the PNAS open access option.

See Commentary on page 11817.

Abbreviation: HSQC, heteronuclear single quantum coherence.

†To whom correspondence may be addressed. E-mail: philipp_selenko@hms.harvard.edu, gerhard_wagner@hms.harvard.edu, or joan_ruderman@hms.harvard.edu.

¶Present address: Cancer Biology and Genetics Program, Memorial Sloan–Kettering Cancer Center, New York, NY 10021.

© 2006 by The National Academy of Sciences of the USA

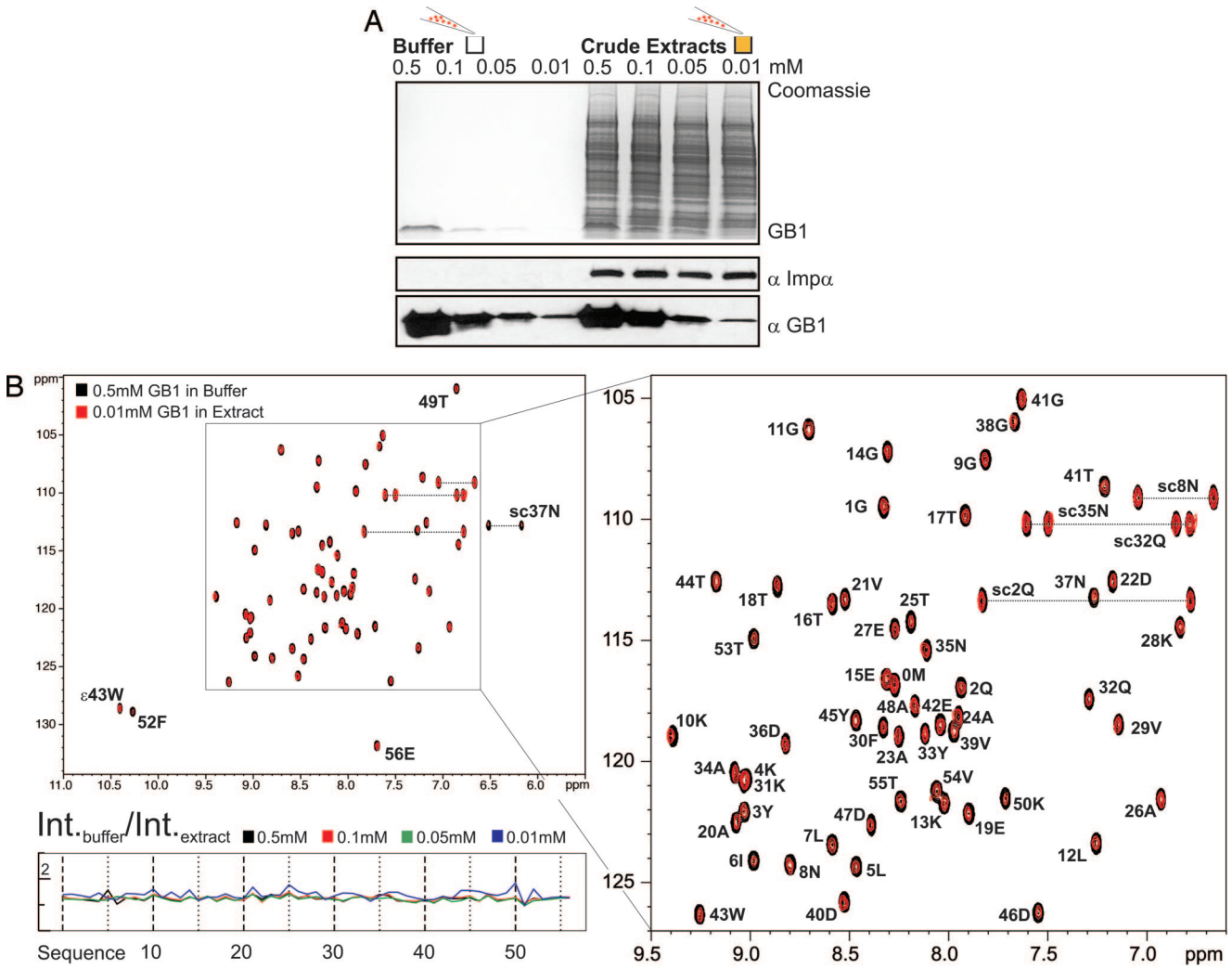

Fig. 1. GB1 in *Xenopus* egg extracts. (*A*) 0.5 μl of SDS/PAGE-separated, Coomassie-stained GB1 buffer and extract NMR samples at the indicated molar concentrations. Low levels of GB1 are readily detected by Western blot analysis using anti-GB1 antibodies (lowest blots). Uniform extract levels of *Xenopus* proteins are exemplified by detection of the endogenous *Xenopus* Importin α polypeptide. (*B*) Overlay of 2D ^{1}H, ^{15}N correlation spectra of purified GB1 (0.5 mM, black, ±2e06 base level for contour display) and of GB1 in crude *Xenopus* egg extracts (10 μM, red, ±0.5e06 base level). These samples are equivalent to the first and last gel lanes, respectively, in *A*. Extract and buffer reference spectra at the indicated molar concentrations were acquired with 16 transients and within 43 min of acquisition time. The graph at the bottom left depicts intensity ratios (buffer over extract) for all GB1 residues and at the indicated sample concentrations.

chemical-shift values were negligibly small (<10 Hz). This result confirmed that the GB1 domain remains identically folded in this environment and does not interact with any of the endogenous components in the extract. The spectral quality of the data also indicated that the overall reduction in signal intensities of individual GB1 residues, compared with pure GB1 samples of the same molar concentrations, was ≈1.5-fold and uniform (Fig. 1*B*). This correlates well with the expected increase in the proteins total correlation time (τ_c) due to cellular viscosity, which has been reported to be on the order of two times of that of water in intact *Xenopus* oocytes (18). The concomitant increase in proton line-widths by an average factor of 1.3 further supports this conclusion (Table 1, which is published as supporting information on the PNAS web site). Moreover, these ratios remained unchanged irrespective of the molar concentrations (10–500 μM) of labeled GB1 (Fig. 1*B*), indicating the overall feasibility of high-resolution NMR measurements at low sample concentrations in *Xenopus* egg extracts.

For in-cell NMR measurements in oocytes, we used a robotic injection device that ensured the highest consistency in cellular sample deposition, both in terms of localization and quantity, and facilitated the most reproducible injection routines (19). Oocytes were placed in 96-well plates and manipulated in a high-throughput fashion, within a minimum amount of time (<2 min per plate) and with no error-prone manual interference. An overview of this injection set-up is given in Fig. 4, which is published as supporting information on the PNAS web site. Automatically injected oocytes were consistently more viable than manually injected counterparts and displayed reduced signs of incision. The quality of the experimental readout by NMR measurements was identical to manually injected cells (data not shown). Two hundred oocytes were used for the final in-cell NMR samples, which corresponded to ≈250 μl of settled cells and, inside a Shigemi NMR tube, sufficed to span transmitter- and receiver-coil extensions of the NMR spectrometer probe (Fig. 2*A Inset*). Ten microliters of ^{15}N-enriched GB1, at injection volumes of 50 nl per cell, was required for the respective in-cell NMR samples. After injections, ^{15}N-GB1 consistently yielded high-quality 2D correlation spectra, even for low intracellular levels of labeled sample (50 μM) and short acquisition times (90 min, 32 scans). Chemical-shift values closely matched those of the pure reference state, although some peaks displayed a distorted, split appearance, which could be caused by different intracellular

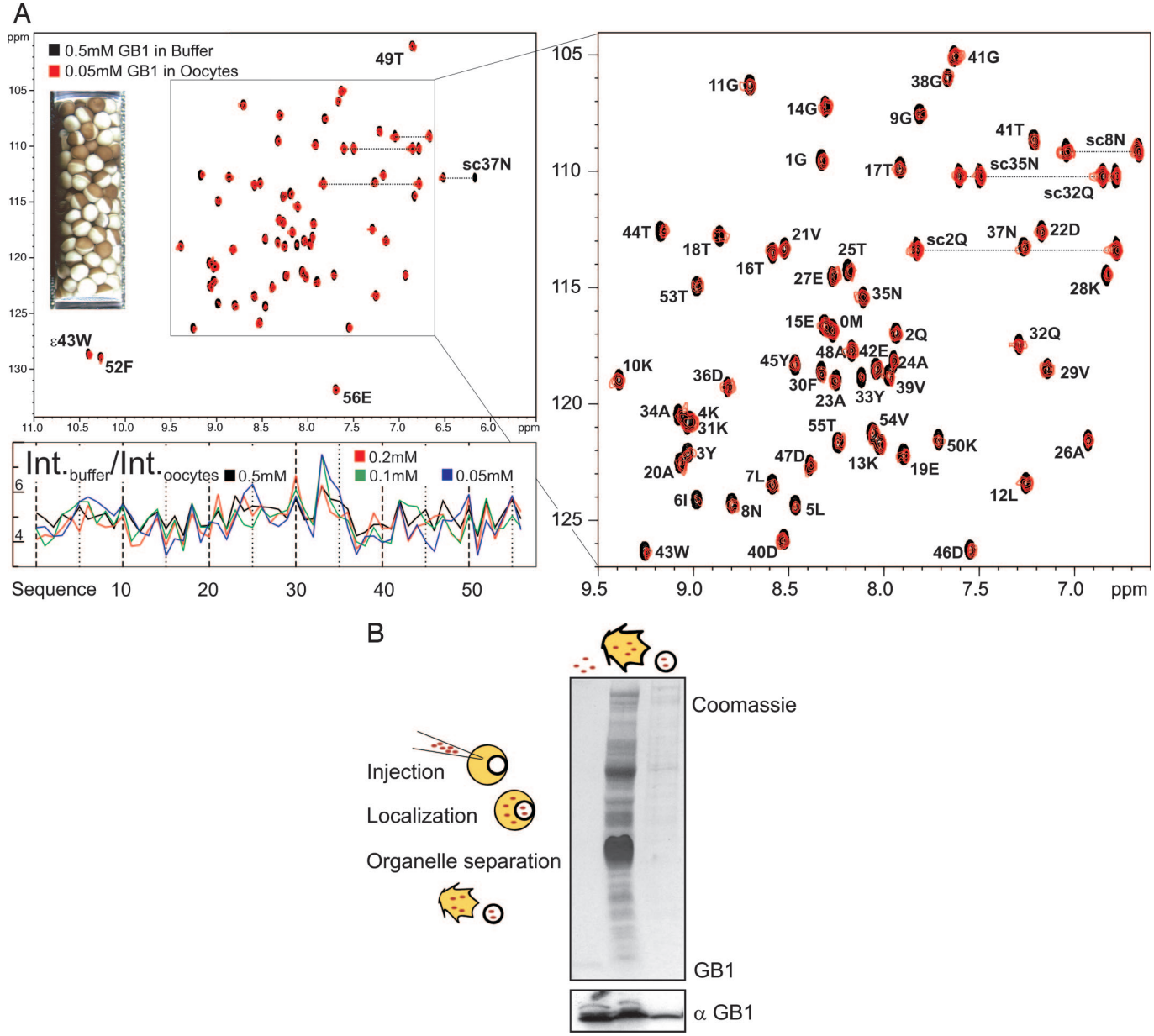

Fig. 2. GB1 in *Xenopus* oocytes. (*A*) View of a typical in-cell NMR sample of 200 oocytes in a Shigemi NMR tube and overlay of the 2D ^{1}H, ^{15}N correlation spectra of purified GB1 (0.5 mM, black, ±2e06 base level for contour display) and of GB1 in *Xenopus* oocytes (50 μM intracellular concentration, red, ±0.05e06 base level). In-cell oocyte and buffer reference spectra at the indicated molar concentrations were acquired with 32 transients and within 90 min of acquisition time. The graph at the bottom left depicts intensity ratios (buffer over oocytes) for all GB1 residues and at the indicated sample concentrations. (*B*) Outline of the single-oocyte enucleation and GB1 quantification experiment. Fifty nanoliters of GB1 (1 mM) were injected into the cytoplasm of individual oocytes and allowed to dissipate for ≈3 h (50 μM intracellular concentration). Because of its small size, unrestricted passage into the nuclear organelle resulted in equilibrium concentrations of GB1 in these two separable compartments. A single oocyte was microdissected to yield the nuclear and cytoplasmic cell fractions, which were separated by SDS/PAGE and analyzed by Western blotting. The first gel-lane displays a 50-nl injection-input control, directly applied for comparison. Detection with anti-GB1 antibodies (lowest blots) indicates quantitative recovery of the injected sample in these two cell compartments.

environments experienced by GB1 (Fig. 2*A*). Indeed, manual dissection of single oocyte nuclei from cytoplasm followed by immunoblotting revealed GB1 protein in both the cytoplasm and the nucleus (Fig. 2*B*). No GB1 was recovered in the concentrated, surrounding solute (data not shown), demonstrating the sealed nature of this cellular system with respect to the injected protein. The average GB1 amide resonance signal intensity in these experiments was reduced ≈5-fold, with an overall increase in proton line-widths by a factor of ≈2.5 (Table 1), when compared with spectra of equimolar, pure GB1 (Fig. 2*A*). Because of the aforementioned distortions in some peak-shapes, these values represent upper-limit estimates. Additionally, the nonlinear nature of these alterations is likely due to an overall signal loss by the inhomogeneous nature of the samples, its effect on the homogeneity of the magnetic field, and the resulting shim/pulse imperfections. These ratios remained unchanged, irrespective of the range of cellular concentrations (50–500 μM) tested (Fig. 2*A*), arguing that these values represent true experimental benchmarks for this system.

The 2D correlation spectra of GB1 allow evaluation of both the global structural hallmarks of the entire domain and the differential line-broadening effects of individual residues, which can be correlated to their structural and dynamic context. In

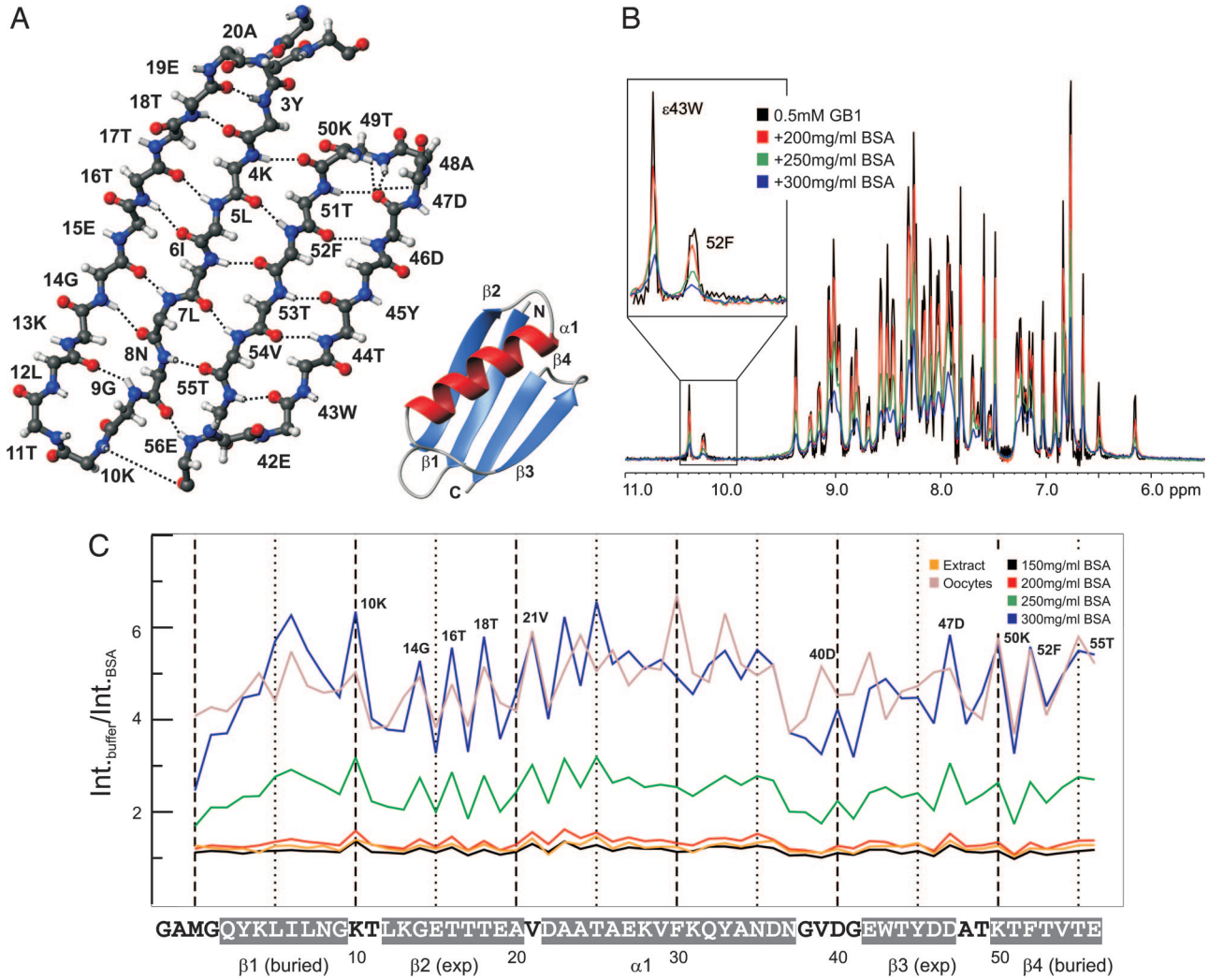

Fig. 3. GB1 in BSA-crowded solutions. (*A*) A ribbon representation of the GB1 domain and the hydrogen-bond network underlying the β-sheet structure are depicted in the same orientation. The α-helix and side-chain moieties are removed for clarity in *Left*. (*B*) Overlay of 1D ^{1}H, ^{15}N correlation spectra of 0.5 mM GB1 (black) and of 0.5 mM GB1 supplemented with 200, 250, and 300 mg/ml (red, green, and blue) of BSA (128 scans with 1,024 points). Characteristic levels of line-broadening and overall signal reduction are readily visible. (*C*) Intensity ratios extracted from 2D HSQC experiments, buffer over BSA-crowded solutions, for all GB1 residues and for BSA concentrations of 150–300 mg/ml. Additionally, extract and oocyte intensity ratios for the respective GB1 samples at 100 and 200 μM are indicated in orange and brown, respectively.

general, we found that hydrogen-bonded amide groups of amino acids in secondary structure elements exhibited greater degrees of signal reduction or, conversely, a higher amount of line broadening than those in unstructured, loop regions. In particular, amide groups of β2 (residues 12–20) and the beginning of α1 (residues 22–37) showed a characteristic pattern of alternating signal reduction ratios, in which spin systems that are solvent-exposed appear less affected by the cellular environment than those residues that are hydrogen-bonded (Fig. 3 *A* and *C*). This paradigm extended to the amide groups of loop residues Lys-10 and Asp-40, which are both hydrogen-bonded to the carboxyl moiety of the most C-terminal residue, Glu-56. Intriguingly, the solute-facing β2 strand of the GB1 domain has been reported to exhibit the highest degree of internal mobility of all secondary structure elements, in the pure state (20). Because peak intensities of individual NMR signals also scale with the internal dynamics of the respective spin systems, for the β2 strand of GB1 this could indicate a more pronounced reduction in mobility upon intracellular localization. These observations suggest that the cellular environment affects the relaxation properties of interior amide groups involved in intramolecular interactions more strongly than those that are solvent-exposed. This interpretation is consistent with the notion that packed internal amides relax primarily via the overall rotation of the protein, whereas solvent-exposed groups experience additional segmental motions. Although cellular crowding significantly affects overall tumbling, it seems to have less of an effect on the small motions of exposed amide groups.

To investigate whether this cellular behavior represents a general feature of a macromolecular-crowded environment toward the folded protein structure, we performed comparative *in vitro* analyses with 0.5 mM ^{15}N-GB1 in buffers containing 150–300 mg/ml BSA (Fig. 3*B*). GB1 NMR signal parameters of the 150 mg/ml BSA sample were found to most closely resemble the functional characteristics yielded by our extract experiments (Fig. 3*C*). Indeed, the overall extract profile of signal intensity ratios closely matched the one obtained in this artificially crowded environment. At higher concentrations of BSA (200–300 mg/ml), we noticed a further decrease in GB1 signal intensities, 1.36- to 4.77-fold, respectively (Fig. 3*C*), with a concomitant increase in proton line-widths by a

factor of 1.5–2.4 (Table 1). Again, these values were consistent with the experimental NMR parameters obtained for GB1 in intact oocytes. Moreover, the pattern of changes in GB1 signal intensity ratios at 300 mg/ml BSA qualitatively and quantitatively corresponded to the observed ratios in whole cells. We can thus conclude that these features appear to constitute a more general characteristic of the intracellular environment toward the folded GB1 structure, which can be similarly mimicked by an artificially crowded solution.

Discussion

The major findings and implications of this work are the following. First, we have demonstrated the experimental feasibility of high-resolution NMR measurements in the complex environments of crude *Xenopus* egg extracts. These extracts are especially suited to predicting a protein's cellular behavior in a conveniently accessible, homogenous solution that closely resembles the cytoplasmic properties of intact cells. Extract NMR measurements may be used to indicate the likelihood for satisfactory in-cell NMR experiments and/or may serve to independently analyze structural and functional aspects of a protein's biological activities in a cell-free setting. Because egg extracts are easily prepared in large quantities and because most biological reactions are executed with comparable activities in these *ex vivo* mixtures, we wish to strongly emphasize their supplementary potential for "cellular" NMR analyses. Moreover, these extracts can be selectively depleted of individual cellular components or supplemented with recombinant proteins, small-molecule inhibitors, and other components, allowing NMR analyses under defined cellular conditions.

Second, we have delineated the methodological reference conditions for quantitative in-cell NMR experiments in intact, living *Xenopus* oocytes. In-cell NMR experiments for the GB1 domain in injected, loosely packed oocytes, at 295 K (23°C) and at intracellular sample concentrations <700 μM, were feasible for up to 8 h, without cells displaying signs of apoptosis. Egg extracts were typically less stable at this temperature and exhibited precipitation after $\approx$3 h. Although these time restrictions preclude many triple-resonance experiments or measurements of dynamics by standard means, the ability to achieve a high degree of sample reproducibility may make it possible to resolve this problem by using multiple identical samples and reference scans. Alternatively, recent methodological advancements in speeding-up multidimensional NMR experiments have proven to be particularly useful for in-cell NMR applications (21). In general, the concentrations of injected proteins needed for the minimally sufficient experimental NMR readout must be determined empirically for each protein, because its size, its expected cellular activity, and type of labeling will critically influence this parameter. As a good approximation, we find that initial experiments in crude *Xenopus* egg extracts, rather than intact living oocytes, yield reasonable lowest-limit estimates for this concentration and allow accurate predictions toward the feasibility of in-cell NMR measurements at physiologically relevant protein levels. We have thus far used injection concentrations in the range of 0.5–10 mM for various labeled protein samples and for in-cell experiments on 600-MHz, cryo-probe-equipped NMR spectrometers. A dilution factor of $\approx$20, because of the intracellular volume of a single oocyte cell ($\approx$1 μl), results in average cellular concentrations of labeled compounds in the range of 25–500 μM. Although these quantities are within the physiological range of many endogenous *Xenopus* proteins, the required injection concentrations will not be achievable for all recombinant proteins or generally suffice for a satisfying experimental readout, especially for biomolecules with promiscuous binding activities toward endogenous cellular components, and within a reasonable amount of experimental time. Clearly, factors like sample solubility and viscosity will critically influence the technical feasibility of the envisaged in-cell NMR experiment and the biological relevance of its outcome. It is evident that a compromise between the experimentally achievable signal-to-noise ratio, the duration of individual NMR experiments, as well as the final concentration of labeled proteins and its physiological relevance will have to be found if these in-cell NMR measurements are to yield biologically meaningful results.

Third, we could directly correlate in-cell NMR parameters of the GB1 domain to *in vitro* NMR data of GB1 in artificially crowded solutions. Results from these experiments indicate that the native intracellular environment of *X. laevis* oocytes and solutions of 250–300 mg/ml BSA exert similar effects on GB1's dynamic and conformational properties. We observe differential alterations in the relaxation behavior of hydrogen-bonded versus non-hydrogen-bonded amide groups in the oocyte environment, which are similarly displayed in crowded *in vitro* solutions. From these data we conclude that GB1's *in vivo* behavior in intact oocytes is governed by intracellular viscosity and the macromolecular composition of the cellular environment.

In other, unpublished work, we have successfully collected in-cell NMR spectra on proteins of larger sizes and with increasingly complex biological activities. We are particularly intrigued by the potential application of this method to investigate post-translational protein modifications *in situ*. These modifications induce significant conformational and functional effects but without a substantial increase in the molecular mass and the ensuing decrease in the spectral quality of the modified protein under investigation. In summary, in-cell NMR approaches in *X. laevis* oocytes and egg extracts offer a multitude of opportunities for structural and functional analyses in a eukaryotic cellular setting and will enable a variety of biological investigations.

Materials and Methods

Plasmid Construction and Protein Expression and Purification. DNA comprising the B1 domain of the streptococcal protein G (residues 374–427) was cloned via NcoI/KpnI sites into a modified pET9d plasmid containing an N-terminal 6× His-tag, followed by a tobacco etch virus (TEV) protease cleavage site. The resulting protein construct exhibits an additional N-terminal GAMGQ-peptide moiety at position -2 to $+2$, as compared with the published GB1 structure (17), after TEV cleavage. ^{15}N-labeled, recombinant GB1 was expressed in *E. coli* BL21 (DE3), grown in minimal medium supplemented with ^{15}N-NH_4Cl as the sole nitrogen source. Cultures were propagated to an OD_{600} of 0.6 at 37°C and then shifted to 28°C for induction with 1 mM IPTG and subsequent growth for 12 h. After cell lysis by sonication, labeled GB1 was initially purified via a Ni-NTA column and eluted with 300 mM imidazole with subsequent His-tag cleavage by addition of TEV protease. The resulting mixture was further purified by means of size-exclusion chromatography equilibrated in 20 mM potassium phosphate buffer/150 mM NaCl at pH 6.4. ^{15}N-GB1 was concentrated to 1–10 mM stock solutions.

Preparation of *Xenopus* Egg Extracts. Crude cytoplasmic extracts were prepared essentially as described in ref. 14. Briefly, female frogs were primed with pregnant mare serum gonadotropin (0.5 ml of 200 units/ml PMSG) and induced to lay eggs 2 days later by injection of human CG (0.5 ml of 1,000 units/ml human CG). Eggs were collected and washed in MMR buffer (100 mM NaCl/2 mM KCl/1 mM $MgCl_2$/2 mM $CaCl_2$/0.1 mM EDTA/5 mM Hepes, pH 7.8). De-jellying was achieved with XB buffer (100 mM KCl/0.1 mM $CaCl_2$/1 mM $MgCl_2$/10 mM potassium Hepes, pH 7.7/50 mM sucrose) supplemented with 2% (wt/vol) cysteine. Subsequently, eggs were washed in XB buffer containing 2 mM $MgCl_2$ and 5 mM EGTA (CSF-XB) and transferred into polypropylene centrifugation tubes with 1 ml of CSF-XB, cytochalasin B and protease inhibitors leupeptin, pepstatin A, and chymostatin (LPC) at 10 μg/ml. Cells were packed by

spinning for 1 min at 400 × *g* and then crushed at 12,000 × *g* for 15 min. The crude interphase extract was removed by piercing the side of the tube with an 18-gauge needle attached to a 5-ml syringe. Extracts were frozen in liquid nitrogen and stored at −80°C for later use.

***Xenopus* Oocyte Microinjections.** Oocytes were prepared essentially as described in ref. 3. Female frogs were anesthetized with 2 g/liter MS-222, and complete ovary lobes were surgically removed to OR2 buffer (82.5 mM NaCl/2.5 mM KCl/1 mM $MgCl_2 \cdot 6H_2O$/5 mM Hepes, pH 7.6). After washing in OR2, ovaries were incubated in collagenase solution [OR2 supplemented with 5% (wt/vol) collagenase, 1% (wt/vol) trypsin inhibitor, and 1% (wt/vol) BSA] for ≈2 h at 18°C on a shaking platform. Cells are washed in OR2 and ND96 (96 mM NaCl/2 mM KCl/1.8 mM $CaCl_2 \cdot 2H_2O$/1 mM $MgCl_2 \cdot 6H_2O$/5 mM Hepes, pH 7.6). Healthy-looking, stage-VI oocytes were sorted out manually and seeded by sedimentation into 96-well plates, pre-adjusted with 150 μl of ND96 buffer per well, for automated injections. Cells were allowed to adhere and recover for 12 h at 18°C before microinjection.

Automatic injections were performed according to the manufacturer's instructions with pre-pulled injection needles (Multi Channel Systems 38GC100TF-10; nozzle aperture ≈15 μm) and with settings of 0.1 bar holding pressure, 0.7 bar injection pressure, 200 ms injection time, and 500 μm injection depth, which corresponds to calibrated sample volumes of 50 nl per oocyte per injection (SD ±10% or ±5 nl). After injection, oocytes were transferred to glass dishes, washed thoroughly with excess volumes of ND96, and allowed to recover for at least 3 h.

Extract, In-Cell, and BSA-Supplemented NMR Sample Preparation. Extract samples were prepared by resuspending 25 μl of a ^{15}N-labeled stock solution of GB1 (in 20 mM potassium phosphate buffer, pH 6.4/150 mM NaCl) and 25 μl of D_2O in 200 μl of crude egg extracts. This yielded final NMR sample volumes of 250 μl, containing 10% D_2O and the respective molar concentrations of GB1. By this procedure, the overall extract dilution factor was kept constant and uniformly small (20%). Extract samples were applied to Shigemi NMR tubes for measurements.

After the final oocyte wash (see above) and 30 min before in-cell NMR sample preparation, oocytes were transferred to ND96 buffer containing 10% D_2O. A Shigemi NMR tube was filled with ND96/D_2O buffer, and cells were settled by gravity with occasional swirling to ensure optimal settling and packing. Two hundred oocytes were used for individual in-cell NMR samples. BSA samples were prepared as follows. A saturated solution of BSA was made in 20 mM potassium phosphate buffer (pH 6.4)/150 mM NaCl and concentrated to 380 mg/ml BSA. Dilutions of ^{15}N-labeled GB1 and this stock solution yielded the final 150–300 mg/ml BSA-supplemented 250 μl of 0.5 mM GB1 NMR samples.

NMR Measurements and Analysis. All experiments were recorded on a Bruker AVANCE 600-MHz NMR spectrometer equipped with a cryo-probe and at 295 K. $^1H\{^{15}N\}$ heteronuclear single quantum coherence (HSQC) correlation spectra were acquired by using a watergate version of a standard, sensitivity-enhanced HSQC pulse-sequence. Extract data were recorded with 16 transients and 1,024(^1H) × 64(^{15}N) complex points for the 2D HSQCs. One-dimensional versions of the HSQC experiments were acquired with 128 scans and 1,024 points. Oocyte data were acquired with 32 transients and 1,024(^1H) × 64(^{15}N) complex points for 2D experiments. The respective reference experiments of pure samples in NMR buffer were obtained with identical spectrometer settings. For proton line-width analyses, 2D spectra were processed without the application of an apodization function in order not to introduce artificial line-broadening. NMR peak parameters, like signal intensities, background noise, and chemical-shift values, were independently extracted and analyzed with XEASY (22) (absolute maximum mode) and NMRDraw (23) (Gaussian fitting within the nlinNLS routine), employing built-in, automated routines for peak identification and picking. Intensity ratios were computed as $[\text{Int.}]_{\text{buffer}}/[\text{Int.}]_{\text{extracts/oocytes}}$; ratios of proton line-widths were calculated as $[\text{LW}]_{\text{extracts/oocytes}}/[\text{LW}]_{\text{buffer}}$; and changes in chemical-shift values, upon extract suspension or oocyte injection, were determined with $\Delta\delta_{\text{total}} = \sqrt{\{\Delta\delta_{1H}\}^2 + \{\Delta\delta_{15N}\}^2}$, in Hz.

Biochemical Analyses. SDS/PAGE separations, membrane transfer, and Western blotting for extract and oocyte analyses were performed according to standard protocols. Anti-GB1 antibodies were obtained from Abcam (ab6678) and used at a 1:5,000 dilution, in TBS, supplemented with 1% Tween 20 and 1% BSA. Anti-Importin α antibodies were a kind gift from D. Görlich (Zentrum für Molekulare Biologie Heidelberg, Heidelberg, Germany). Single-oocyte enucleation was performed manually by using a dissecting microscope. The nucleus was directly applied to SDS sample buffer; the crude cytoplasmic fraction of the remaining oocyte was collected by centrifugation in a glass capillary and resuspended in sample buffer without further purification.

We thank Matthew Dedmon of the G.W. laboratory for valuable discussions on this project and for carefully reading the manuscript. We are also grateful to Eunah Chung and Michael Yan Jia Lai of the J.R. laboratory for support in all *X. laevis*-related practical aspects of this work. P.S. is a Human Science Frontier Program Organization Long-Term Fellow (LT00686/2004-C), Z.S. is supported by a Beckman research fellowship, and B.G. was supported by National Cancer Institute Training Grant T32CA09361. This work was additionally funded by National Institutes of Health Grants GM47467 (to G.W.) and HD23696 (to J.R.).

1. Sali, A., Glaeser, R., Earnest, T. & Baumeister, W. (2003) *Nature* **422,** 216–225.
2. Serber, Z., Corsini, L., Durst, F. & Dötsch, V. (2005) *Methods Enzymol.* **394,** 17–41.
3. Serber, Z. & Dötsch, V. (2001) *Biochemistry* **40,** 14317–14323.
4. Dedmon, M. M., Patel, C. N., Young, G. B. & Pielak, G. J. (2002) *Proc. Natl. Acad. Sci. USA* **99,** 12681–12684.
5. Hubbard, J. A., MacLachlan, L. K., King, G. W., Jones, J. J. & Fosberry, A. P. (2003) *Mol. Microbiol.* **49,** 1191–1200.
6. McNulty, B. C., Young, G. B. & Pielak, G. J. (2006) *J. Mol. Biol.* **355,** 893–897.
7. Serber, Z., Straub, W., Corsini, L., Nomura, A. M., Shimba, N., Craik, C. S., Ortiz de Montellano, P. & Dötsch, V. (2004) *J. Am. Chem. Soc.* **126,** 7119–7125.
8. Wieruszeski, J. M., Bohin, A., Bohin, J. P. & Lippens, G. (2001) *J. Magn. Reson.* **151,** 118–123.
9. Bryant, J. E., Lecomte, J. T., Lee, A. L., Young, G. B. & Pielak, G. J. (2005) *Biochemistry* **44,** 9275–9279.
10. Burz, D. S., Dutta, K., Cowburn, D. & Shekhtman, A. (2006) *Nat. Methods* **3,** 91–93.
11. Murray, A. W. (1991) *Methods Cell Biol.* **36,** 1–718.
12. Kay, B. K. (1991) *Methods Cell Biol.* **36,** 663–669.
13. Liu, X. S. & Liu, X. J. (2006) *Methods Mol. Biol.* **322,** 31–43.
14. Evans, J. P. & Kay, B. K. (1991) *Methods Cell Biol.* **36,** 133–148.
15. Murray, A. W. (1991) *Methods Cell Biol.* **36,** 581–605.
16. Crane, R. & Ruderman, J. (2006) *Methods Mol. Biol.* **322,** 435–445.
17. Gronenborn, A. M., Filpula, D. R., Essig, N. Z., Achari, A., Whitlow, M., Wingfield, P. T. & Clore, G. M. (1991) *Science* **253,** 657–661.
18. Sehy, J. V., Ackerman, J. J. & Neil, J. J. (2002) *Magn. Reson. Med.* **48,** 42–51.
19. Schnizler, K., Kuster, M., Methfessel, C. & Fejtl, M. (2003) *Recept. Channels* **9,** 41–48.
20. Barchi, J. J., Jr., Grasberger, B., Gronenborn, A. M. & Clore, G. M. (1994) *Protein Sci.* **3,** 15–21.
21. Reardon, P. N. & Spicer, L. D. (2005) *J. Am. Chem. Soc.* **127,** 10848–10849.
22. Bartels, C., Xia, T.-H., Billeter, M., Guntert, P. & Wüthrich, K. (1995) *J. Biomol. NMR* **5,** 1–10.
23. Delaglio, F., Grzesiek, S., Vuister, G. W., Zhu, G., Pfeifer, J. & Bax, A. (1995) *J. Biomol. NMR* **6,** 277–293.